SPACE RESEARCH COORDINATION CENTER

THE ATOM-MOLECULE REACTION
$D + H_2 \rightarrow HD + H$
STUDIED BY MOLECULAR BEAMS

BY

J. GEDDES, H. F. KRAUSE, AND W. L. FITE

SRCC REPORT NO. 165

UNIVERSITY OF PITTSBURGH
PITTSBURGH, PENNSYLVANIA

FEBRUARY 1972

The Atom-Molecule Reaction $D + H_2 \rightarrow HD + H$ Studied by Molecular Beams[*]

J. Geddes[†], H. F. Krause[‡], and W. L. Fite
Department of Physics
University of Pittsburgh
Pittsburgh, Pennsylvania 15213

Abstract

Collisions between deuterium atoms and hydrogen molecules have been studied in a modulated crossed beam experiment. The relative signal intensity and the signal phase for product HD from reactive collisions allowed determination of both the angular distribution and HD mean velocity as a function of angle. From these a relative differential reactive scattering cross section in center-of-mass coordinates was deduced. The experiment indicates that reactively formed HD having little or no internal excitation departs from the collision anistropically, with maximum amplitude 180° from the direction of the incident D beam in C-of-M coordinates, which shows that the D-H-H reacting configuration is short-lived compared to its rotation time. Non-reactive scattering of D by H_2 was used to assign absolute values to the differential reactive scattering cross sections.

---

[*] This Research was supported in part by the National Aeronautics and Space Administration under Grant No. NGL 39-011-013.

[†] Present Address: The Queen's University of Belfast, Belfast, North Ireland.

[‡] Present Address: Oak Ridge National Laboratory, Oak Ridge, Tennessee, 37830

I. INTRODUCTION

The pioneering work of Taylor and Datz[1] in 1955 on the reaction $K + HBr \rightarrow KBr + H$ demonstrated that crossed beam techniques could be applied successfully to the study of thermal energy chemical reactions. It was immediately clear that with this experimental method the means of investigating the dynamics of bimolecular chemical reactions were within reach, at least for the alkali species and their salts, where use could be made of surface ionization detectors with high efficiency and specificity. Very quickly other laboratories[2] took up the challenge of thermal energy reactive scattering experiments and with improved techniques began to isolate the experimental parameters of interest. Consequently, for thermal energy reactions involving alkali species much detailed information is available about both the angular and velocity distribution of the products, the lifetime of the intermediate collision complex, the activation energy, the variation of reaction cross section with energy and the internal energy states of the products. All this accumulated data leads to an understanding of the ionic bonding mechanism, this being dominant in alkali salts.

For non-alkali species, where the bonding is covalent, until recently a very limited amount of success had been achieved in thermal energy neutral-neutral reactive scattering experiments. Here a detector that is "universal" in nature is required. Such a detector has been in use widely in beam experiments and it employs electron impact ionization followed by mass analysis. The inherent disadvantages of this detection system are both the low efficiency and the inability to distinguish between reactively scattered beam molecules and background gas molecules of the same species.

The early partly successful experiments using universal detectors were on the reaction D + H_2[3] and H + D_2.[4] The small rate constant and the high background pressure of the interfering species, together with the detector's limitations, made meaningful experimentation extremely difficult. Improvement of the design of universal detectors and the use of elaborate differential pumping around the ionizer has led to reduction of the interfering background, and recently several laboratories have reported[5] on investigations of reactions of the type D + Br_2 and Cl + Br_2.

One reactive scattering system, that of hydrogen atoms by hydrogen molecules $H + H_2 \rightarrow H_2 + H$ or its isotopic variants, is of fundamental importance from a chemical kinetics viewpoint. The elementary character of this bimolecular reaction makes it an excellent testing ground for theories of chemical reaction. It has been the object of many theoretical investigations, the most recent and comprehensive of which have been by Karplus and co-workers,[6] and by Micha.[7]

Experimental progress in investigating this reaction has been slow. The bulk reaction rate constant was measured as a function of temperature as early as 1930 for para- to ortho-hydrogen conversion due to atomic hydrogen.[8] In the last decade the other hydrogen isotopic reactions have been investigated by several workers[9] using various techniques to determine the reaction rate in the temperature range 250°K to 750°K. These experiments have provided much needed bulk information about this reaction. However, at best, given a particular set of reaction model assumptions, the data can determine only rigorous bounds on integrated properties of the cross section.[10]

The preliminary crossed beam scattering experiments on the hydrogen exchange reaction[3,4] had been unable to make use of the full potential of this powerful technique. The present paper describes the progress made recently towards further understanding the reaction $D + H_2 \rightarrow HD + H$. To this end measurements have been made of the HD differential scattering cross section, the velocity of the products and, for calibration purposes, the differential scattering cross section for non-reactive scattering of D on H_2.

II. KINEMATICS

In crossed beam experiments it is of value to construct a velocity vector diagram of in-plane scattering. Figure 1 shows such a diagram of the $D + H_2$ reaction at threshold energy with the molecular beam cooled, as was the case in these experiments, to ensure that only low lying rotational states participate in a collision.

The velocity of the H_2 molecule OK is the mean velocity of a H_2 beam cooled to 77°K. The D atom velocity OB is that which makes the relative kinetic energy correspond to the activation energy 0.33 eV.[11] OC_R represents the center-of-mass velocity. Applying conservation of momentum to the reaction and assuming the initial H_2 and product HD have no internal energy, the circle designated HD_R is found to be the locus of velocities of HD product in the center-of-mass coordinates. The ratio of the radius of this circle to the D atom speed in center-of-mass coordinates is $[\frac{1}{3} (1 - \frac{\Delta E}{E})]^{1/2}$ where ΔE is the endothermicity and E the relative kinetic energy. The tangents drawn from the origin to this circle OH and OH' represent the angular limits between which reactive HD signals will be observed, approximately from a laboratory angle of +41½° to -28½°. (The positive sign is used to denote deflection from the D direction towards the H_2 cross beam direction.) Within these limits at a laboratory angle β the HD product has two separate velocity components, OD and OM corresponding to backward and forward scattering in the center-of-mass system.

Recognition must be taken at this point of the almost certain presence of HD molecules in the D atom beam[3,4] due to the difficulty of separating the impurity HD from the D_2 feeder gas. The velocity vector diagram for HD elastic scattering from H_2 is also shown in Fig. 1. OA represents the mean velocity of HD from a furnace running at a typical temperature for D beam production (2800°K). The circle HD_{sc} is the locus of scattered HD velocities in the center-of-mass system. In this idealized case scattering is between laboratory angles approximately +50° to -36°.

This is approximately the same angular range as for reactive scattering. At each laboratory angle there can be reactive and non-reactive contributions from forward and backward scattering in the center-of-mass coordinates. With these similarities in angular distribution it is important to distinguish experimentally between reactive collisions and scattering of impurity HD.

III. APPARATUS

A. General Description

The apparatus used in this experiment is illustrated diagrammatically in Fig. 2. The deuterium atom beam source was a tungsten furnace operating at up to 3000°K in the first of three differentially-pumped chambers. In the second chamber the beam was modulated by a rotating toothed chopper wheel. After entering the third chamber, this beam passed through a liquid helium cryopumped fourth chamber, within which the dc H_2 beam crossed the modulated D beam. HD formed by reaction emerged from the fourth chamber and was collimated into a beam for detection. The detector was a high efficiency ionizer (10 mA/Torr), which responded to number density of molecules in the beam, followed by an Extranuclear Laboratories quadrupole mass filter and particle multiplier. The ionizer was enclosed in a titanium-getter-pumped fifth chamber to reduce the partial pressure of background gas which is a severe source of shot noise. All of this assembly rotated about the beam intersection point in the plane of the two crossed beams within $\pm 50^{\circ}$ of the D beam axis. Neither beam was velocity selected and the effective kinetic temperature of the reactants in the center-of-mass coordinates was in a very narrow range just below 1500°K. Lock-in circuitry was used and the modulation frequency ranged from 1440 through 9400 Hz.

B. Performance

1. Atomic Beam

Since the atomic beam intensity from a low pressure thermal dissociation furnace is very limited, the source-to-interaction-region distance was made as small as practicable, 8 cm, in order to achieve high atom density. Besides this limitation on intensity the deuterium atom beam presented several major difficulties.

First, the molecular deuterium from which the D atoms were produced contained a 0.3% HD impurity. Although dissociation ran around 95%

the undissociated HD impurity could, on non-reactive scattering from the H_2 target, give a modulated HD signal comparable with that expected from HD formation in the reaction.

A second problem caused by the D beam arose with its termination in the third chamber. Residual gas analysis of the associated pressure increase of 3×10^{-7} Torr indicated that a large fraction of it is due to HD molecules. Presumably, at walls of the third chamber, the D atoms undergo surface reactions in which hydrogen is abstracted from adsorbed gases. This background introduced severe shot noise in the detector when modulated HD was being observed.

2. Molecular Beam and Fourth Chamber

The H_2 beam was contained within the double walled fourth chamber which was suspended from the lid of the third chamber. The multichannel nozzle through which the H_2 issued was attached thermally to the liquid nitrogen cooled outer shroud of the fourth chamber so that the temperature of the H_2 beam was approximately 77°K. Additional collimation of the beam was found to be necessary and was provided by an aperture in the liquid helium cooled plate shown in Fig. 2. The very dense H_2 beam after traversing the interaction region was removed through condensation on the opposite liquid helium cooled surface. To avoid problems with the formation of "hydrogen ice" and the subsequent reduction in sticking probability for H_2, a trap was constructed to increase the effective surface area of the collection region. With this arrangement H_2 beams, which gave up to 10% attenuation of the D atom beam, could be used for up to six hours with a pressure rise of no more than 5×10^{-7} Torr in the third chamber.

The fourth chamber and its liquid nitrogen-cooled shroud, also had apertures, through which the D beam entered normal to the H_2 beam direction, and large in-plane slots for observation of scattering. For the reactive scattering measurements both beams were 6 mm in diameter at the interaction region and the detector could observe scattering events at angle differing from the detector axis (which passed through the target center) by as much as 3°. This angle was 1° for the non-reactive scattering results, where collimation was tightened.

Because the molecular beam source operated at low temperature and at high pressure ($\sim$ 1 Torr), the possibility that some clustering to form molecular polymers, $(H_2)_n$ might be occurring in the expansion into the vacuum required consideration. In a separate experiment using modulated beam mass spectrometry, dissociative ionization products from processes such as $e + (H_2)_2 \rightarrow H_3^+ + H + 2e$ or $e + (H_2)_3 \rightarrow H_5^+ + H + 2e$ were seen only to be that for normally occurring HD in H_2. We regard the experiment as indication that the cross beam was effectively free of H_2 clusters; otherwise, the mass 3 signals would have been greater and mass 5 signals would have been observable.

3. Detector

Either reaction product, H or HD, could in principle be detected. Experimentally it was found that the dc background of H^+ signal was very much greater than the mass 3 amu signal and consequently the major effort was directed at observing product HD molecules. A significant reduction in the shot noise at mass 3 was achieved by reducing the background pressure in the ionizer. The complete ionizer and quadrupole rods were enclosed in a liquid nitrogen cooled titanium sublimation pump (200 liters/sec for H_2) with only a small aperture into the third chamber through which the beam could be sampled. The background partial pressures of HD and H_2 were reduced to about two orders of magnitude by this arrangement, that of HD to better than 10^{-9} Torr and H_2 to better than 10^{-8} Torr. Under these conditions with an integrating time of 100 seconds the HD signal-to-noise ratio was at best 10 to 1. Reduction in the H_2 background improved the signal-to-noise ratio when scattered D atoms were being detected.

Extreme care had to be taken at all angles to ensure that all modulated D atoms scattered on the H_2 beam passed cleanly through the detection system. Otherwise chemical reaction of the D atoms on surfaces close to the ionizer could give rise to reflected modulated HD molecules which would be detected as a phase-sensitive signal indistinguishable from reactive scattering.

IV. THE TECHNIQUE FOR MEASURING THE HD PRODUCT VELOCITY

Besides measuring the amplitude of the ac signal the lock-in amplifier was used to measure the signal phase. The phase at which the signal appears with respect to the reference signal allows the speed of the neutral particles to be determined from the chopping frequency f and the distance, L, travelled from the modulator to the ionizer.[12] For a monoenergetic beam velocity u the phase shift Φ is given by

$$\Phi = 2\pi fL/u \qquad (1)$$

In the case of square wave modulated Maxwellian beams the phase shifts as well as the amplitude reductions due to smearing as the faster particles at one beam pulse overtake the slower particles of the preceding pulse have been evaluated.[13]

When determining the mean velocity of reactively scattered HD, it is necessary to take into account contributions to the recorded phase shift allowing for the D atom travelling from the chopper to the interaction region (4.8 cm) and the HD from the interaction region to the detector (11.5 cm). When the D atom signal in the primary beam is used as a reference, the difference in flight times of D^+ and HD^+ through the mass filter must also be taken into account.

The HD signal itself would be the superposition of four signals each with a different phase corresponding to the different velocities of the forward and backward scattering components of both elastically scattered HD and reaction product HD. The tuned narrow-band lock-in amplifier responds to the fundamental Fourier component of the modulated signal. Hence the HD signal would be

$$C\, e^{i(2\pi ft - \phi)} = \sum_{n=1}^{4} A_n\, e^{i2\pi f(t - \tau_n)} \qquad (2)$$

where A_n is the amplitude of the n-th velocity component and τ_n represents the flight time from the chopper to the detector. Upon algebraic elimination of the amplitude, C, one can write

$$\tan \phi = \frac{\sum_{n=1}^{4} A_n \sin 2\pi f\tau_n}{\sum_{n=1}^{4} A_n \cos 2\pi f\tau_n} \qquad (3)$$

In the particular case of one of the A_n's being very much larger than the others, the phase change ϕ will be proportional to the chopping frequency f. Linearity of the phase angle with frequency is therefore a test for the predominance of one component. Deviations from linearity indicate the extent to which other velocity components contribute to the signal.

V. MEASUREMENTS

A. Angular Distribution of Reactively Scattered HD

Figure 3 shows the angular distribution in laboratory coordinates of the detected HD reaction product. The error bars represent 90% confidence limits for six experiments on the relative signal as a function of laboratory angle. The absolute differential cross section units on the ordinate were assigned by methods discussed in Section VI. C. below.

The D beam temperature was 2850°K and the modulation frequency 1400 Hz. Signals are not shown at angles less than 15° from the primary beam, where the scattered HD impurity in the D beam becomes significant.

Four tests were applied to distinguish HD reaction product and non-reactively scattered impurity HD. First, the change of HD signal as the furnace temperature was changed was noted; an increase with increasing temperature indicated D atoms reacting, while a decrease indicated scattering of impurity HD, which becomes increasingly dissociated. Data are reported only for those angular ranges where the signals increased with increasing furnace temperature.

Second, the angular distribution of D atoms and D_2 molecules which could only have been non-reactively scattered were compared with observed HD. The observation that the HD angular distribution was markedly different from the distributions of the D and D_2 indicated that the HD was not produced by non-reactive scattering or by HD formed in surface reactions on detector collimating slits by scattered D atoms.

Third, from consideration of the kinematics, including the centroid distribution, the angular range over which the HD was detected was +48° to -35°, which is consistent with reactive scattering but too narrow for elastic scattering.

The fourth test is the most significant one. It involved measuring the mean HD product velocity and considering the kinetics of the reaction.

B. Mean Velocity of Scattered HD

The mean velocities of the HD molecules have been calculated from the phase shifts recorded experimentally. These have been plotted on a velocity vector diagram in Fig. 4. The modulation frequency (7200 Hz) used for the measurements in this figure was a compromise between the high frequency requirement for large, readily measurable phase shifts and the low frequency requirement for minimum loss in signal amplitude due to spreading and smearing of the pulses in the modulated beam. The observed phase shifts, for convenience, were measured with respect to the direct D atom beam signal, and ran from about 50° at small angles down to 10° at the largest laboratory angle.

The dependence of the HD phase angle on frequency was investigated from 1440 Hz to 9400 Hz and was found to be linear at all angles greater than 15 degrees. The scatter of points plus the statistical uncertainty in the measurements, would admit no more than a 10% contribution from velocity components other than a main one.

C. Angular Distribution of Scattered D Atoms

Figure 5 shows the recorded laboratory angular distribution of scattered mass 2 particles over the angular range 4° to 45°, measured from the direction of the D atom beam. Since D and H_2 are indistinguishable in the detector system, the mass 2 signal represents the sum of D scattered by H_2 and H_2 scattered by D. The ordinate of Fig. 5 is given in absolute cross section units assigned as discussed in Section VI. C. below.

It is straightforward to show that if (1) two colliding particles have the same mass, (2) the collision is elastic, and (3) a number density detector is used, then the laboratory angular distribution of each of the colliding species should be symmetrical about the direction of its beam. On the assumption that the scattering cross section consists of an isotropic "hard-sphere" component and a large forward scattered component, it would be expected that the data shown in Fig. 5 would be symmetric about the D beam direction. The observation that deviations from symmetry did not exceed 10% over the specified angular range, indicates that the apparatus was satisfactorily free of misalignments and asymmetries.

VI. ANALYSIS AND DISCUSSION OF RESULTS

A. HD Product Average Velocity

When two beams with number densities n_1 and n_2 intersect at right angles in a volume V, the total number of reactive collisions per second, N, is given by[14]

$$N = n_1 n_2 V \int_0^\infty \int_0^{\pi/2} v\sigma(v) I(v,\Psi) dv d\Psi \qquad (4)$$

where v is the relative velocity, σ(v) is the total cross section for reaction, $I(v,\Psi)$ is the normalized distribution of the relative velocity vectors and coordinate Ψ is the inclination of the relative velocity vector to the n_1 beam.

From Eq. (4) the most probable relative vector velocity for reaction can be found if the dependence of the total cross section on relative velocity is known.

A cross section with simple functional form is now considered. It is assumed that the excitation function is independent of orientation and has a velocity dependence given by

$$\sigma(v) = \begin{cases} 0 & \text{when } v < v_0 \\ \sigma\left(1 - \frac{v_0^2}{v^2}\right) & \text{when } v \geq v_0 \end{cases} \qquad (5)$$

where v_0 is the relative velocity corresponding to the activation energy and σ is a constant. This simple choice introduces no large bias except where noted elsewhere. This $\sigma(v)$ does not differ greatly from that found in the $H + H_2$ semi-classical study by Karplus, Porter and Sharma[6b]. For an activation energy of 0.33[11] eV, the most probable relative velocity vector has coordinates (9.8×10^5 cm/sec, $\beta = 4.5^\circ$).

In Fig. 4, the experimental velocities are shown on a velocity vector diagram constructed using these average values and permitting no change in internal energy. The HD velocities recorded experimentally have been shown to represent just one of the four possible scattering components and as such should fit onto at least part of an appropriate velocity vector diagram. The data fit this diagram and have been shown to be incompatible with elastically scattered HD impurity.[12] These data and the angular distribution width in the laboratory system are also incompatible when endothermicities of reaction are assumed larger than .05 eV (corresponding to changes of rotational energy quantum number of about $\Delta J = 3$). Hence the HD signal is again confirmed as a reaction product and further it is principally back-scattered in the center-of-mass system. The type of analysis carried out above does not predict the dependence of cross section on velocity but only tests a given model.

B. Center-of-Mass Angular Distribution

Of major interest is the determination of the differential reactive scattering cross section in center-of-mass coordinates. This can be related to signals observed in a crossed-beam experiment by a formalism that is well known.[15,16] For a detector with solid angle Ω_D that uses electron impact ionization (and therefore detects number density), the signal observed in the plane of intersection of the two beams at a laboratory angle, β (measured from the direction of the atomic beam) is

$$S(\beta) = Kn_1n_2V \int_{\Psi=0}^{\pi/2} \int_{v=0}^{\infty} vI(v,\Psi)dvd\Psi \int_{\Omega_D} \frac{d\sigma(v,\theta)}{d\Omega} \frac{Q_i}{u(v,\beta,\theta,\Psi)} J(v,\beta,\theta,\Psi)d\Omega_L \tag{6}$$

where

$$J(v,\beta,\theta,\Psi) = \left[\frac{u(v,\beta,\theta,\Psi)}{w(v,\Delta E)}\right]^2 \frac{1}{|\cos \xi|}$$

and

$$\cos \xi = \frac{u^2 + w^2 - v^2/4}{2uw} ,$$

where K is a constant containing fixed apparatus parameters, and u and w are the velocities of the detected product (HD in this case) measured in laboratory and center-of-mass coordinates respectively. The effective or average differential cross section in the center-of-mass coordinates, $\frac{d\sigma}{d\Omega}$ is dependent on v and contains the relative probability of a product moving in a given direction after collision. Q_i is the electron impact ionization cross section of the detected product and the u in the denominator reflects the fact that sensitivity of detection decreases with velocity in laboratory coordinates. The remaining term in the solid angle integral, J, is the usual Jacobian which describes the way infinitesimal solid angles transform between the center-of-mass and laboratory coordinates systems for each point on the center-of-mass scattering circle of a monoenergetic velocity diagram. It is noteworthy that the form of Eq. (6) is appropriate to the assumptions that angular dispersion of the perpendicular beams has been neglected.

For simplicity of analysis it is also assumed that the effective differential cross section is separable in its variables and that

$$\frac{d\sigma(v,\Theta)}{d\Omega} = \sigma(v)f(\Theta) \qquad (7)$$

where $f(\Theta)$ is the normalized angular distribution in center-of-mass coordinates. Since $\sigma(v)$ expressed in Eq. (5) weighted with the kinetic energy distribution of reactants implies an average reaction energy in this experiment of .48 eV and since this kinetic distribution has a width of .1 eV (FWHM), Eq. (7) assumes that $f(\Theta)$ does not vary appreciable with v throughout this range.

The experimental results on the mean velocity of product HD (see Fig. 4) suggest that in this experiment, the reaction proceeds with effectively zero endothermicity, ΔE. If zero endothermicity is assumed, and Eq. (7) is inserted into Eq. (6), it can be shown that the solid angle integral in Eq. (6) is independent of v except for the factorable term $v^{-1}\sigma(v)$. This integral with $Q_i v^{-1}\sigma(v)$ removed and represented as $A(\beta,\Psi)$, is determined once $f(\Theta)$ and Ψ are specified. Equation (6) can then be written as

$$S(\beta) = KQ_i n_1 n_2 V \sum_{\text{all } \Psi_i} a(\Psi_i) A(\beta,\Psi_i) \qquad (8)$$

where

$$a(\Psi_i) = \int_{\Psi_i - \frac{\Delta\Psi}{2}}^{\Psi_i + \frac{\Delta\Psi}{2}} \int_{v=0}^{\infty} \sigma(v) I(v,\Psi) dv d\Psi,$$

$\Delta\Psi$ being the grid size chosen for numerical integration, and

$$A(\beta,\Psi_i) = \int_{\Omega_D} \frac{f(\Theta) J(\beta,\Theta,\Psi_i)}{u(\beta,\Theta,\Psi_i)} d\Omega_L \ .$$

The signals as a function of β have been evaluated numerically using trial forms of $f(\Theta)$ in Eq. (8) with $\Delta\Psi = .5^\circ$. While the trial forms of $f(\Theta)$ are arbitrary, the best fits of the experimental data were obtained using

$$\begin{aligned} f(\Theta) &\propto \cos^N(M(180^\circ - \Theta)), \qquad && |M(180^\circ - \Theta)| < 90^\circ \qquad (9) \\ &= 0 \qquad , && \text{otherwise.} \end{aligned}$$

Figure 6 shows a comparison of the experimental results with those computed using Eqs. (5), (8), and (9). The noteworthy features of this integral are its invariance with respect to change in M in the laboratory region $+5^\circ$ to $+25^\circ$ and its sensitivity over the other regions. The insensitive region is due to the function $f(\Theta)$ remaining relatively unchanged over the center-of-mass region 170° to 190° with respect to changes in M. Furthermore, the large error bars in this region make it difficult to assign a unique form of $f(\theta)$.

In Fig. 7 the most probable experimental differential cross section, $\cos^2(1.35(180^\circ - \theta))$ has been compared (after normalization at 180°) with that derived theoretically by Micha for $D + H_2(J = 1)$ reactive scattering at an energy consistent with this experiment. Agreement is very good from $\theta = 180^\circ$ to 140°. However, beyond this region, where the experimental distribution is extremely sensitive to the form of the scattering cross section, agreement is poor. This result is little changed with the inclusion of Micha's $J = 0$ and $J = 2$ H_2 state solutions weighted to their estimated experimental abundance.

Calculations by Karplus and Tang[6] on the isotopic reaction $H + H_2$ are in broad agreement with the general features of the above results, namely, a strong backward peaking in the center-of-mass angular distribution and a sharp fall off with angle in the experimental energy range.

Figure 8 shows a comparison of the present results with those of Datz and Taylor.[3] The apparent laboratory symmetry of the Datz and Taylor results about 5° is difficult to understand when the asymmetric nature of the center-of-mass to laboratory transformation is considered. However, it is believed that the detector collimation of Datz and Taylor did not permit the detector to view the entire interaction volume when the detector was moved out of the D beam.[17]

C. Calibration of Scattering Cross Sections

For absolute calibration of the reactive cross section, rather than attempt to determine accurately the beam densities and the geometric factors which are contained in the constant K of Eq. (6), the following procedure was used.

Both the reactive HD and non-reactive scattered D were monitored under identical experimental conditions. If the absolute non-reactive differential scattering cross section is known, then the ratio of signals, after correction for ionization cross section and velocity difference, determines the absolute reactive differential cross section, since the beam densities and apparatus parameters remain unchanged.

The first step is to consider the non-reactive scattering. There is a published absolute value of 55 x 10^{-16} cm^2 for the total scattering cross section, σ_e, for H by H_2[18] at mean velocities comparable to those of the present experiment. In the present experiments, there is the complication that D scattered by H_2 and H_2 scattered by D are indistinguishable in the mass spectrometric detector. In order to obtain absolute differential non-reactive scattering cross sections for calibration in the present experiments the following procedure was used.

It is assumed that the absolute differential scattering cross section can be represented by $d\sigma_e/d\Omega = \sigma_e h(\Theta)$, where $h(\Theta)$ is the normalized angular distribution function in center-of-mass coordinates. Application of Eq. (6) gives for the non-reactive scattering signal at the laboratory angle, β, $(\beta = \Theta/2)$

$$\begin{aligned} S(\beta) &= 4Kn_1n_2V\sigma e\Omega_D \left[h(\Theta)Q_D + h(180^\circ - \Theta)Q_{H_2}\right] \\ &= 4Kn_1n_2V\sigma_e\Omega_D(Q_D) \left[h(\Theta) + (Q_{H_2}/Q_D)h(180^\circ - \Theta)\right] \quad (10) \end{aligned}$$

where K is the apparatus constant of Eq. (6), Q_D and Q_{H_2} are the known ionization cross sections for D and H_2 respectively. Knowledge of $h(\Theta)$ is all that is required to determine Kn_1n_2V. (The response of the electron multiplier in the detector to D^+ and H_2^+ is assumed identical.)

The observed scattering signals (Fig. 5) makes it appear that for $20^\circ < \beta < 45^\circ$ ($40^\circ < \theta < 90^\circ$), $h(\theta)$ is constant which suggest that the scattering consists of a forwardly scattered peak plus an isotropic hard-sphere scattering component. It is assumed that this is the case, which is in accord with quantum mechanical studies of this and similar systems[19,6c], and that $h(\theta)$ retains the same constant value at angles $\theta > 90^\circ$.

Subtraction of the assumed hard-sphere component indicates (see Fig. 5) that in the forward direction the cross section has the angular dependence $h(\theta) \propto \theta^{-7/3}$. It is known from theory that for small-angle deflections in a central force potential of the form $V = -C/r^S$ the differential cross section is of the form

$$\frac{d\sigma_e(\theta)}{d\Omega} \propto \theta^{-2(1 + 1/S)} . \qquad (11)$$

The observed angular dependence is that expected for $S = 6$, and identifies the scattering as being caused by a van der Waals force.

At very small angles (dependent on energy), quantum effects take over and the differential scattering cross section loses its 7/3 power dependence and becomes constant. The mean value of this cross-over angle has been estimated as $\theta_C = 2.5^\circ$.[20]

It was thus assumed that $h(\theta)$ had the form

$$\begin{aligned} h(\theta) &= a(1 + b\,\theta^{-7/3}) && 180^\circ > \theta > \theta_C \\ &= a(1 + b\,\theta_C^{-7/3}) && 0 < \theta < \theta_C \end{aligned} \qquad (12)$$

This form was inserted into Eq. (10) and fit to the shape of the experimental data given in Fig. 5, thus determining the constant b of Eq. (12), above. Integration over all angles, θ, and normalizing to unity determined the constant a. Knowledge of the total cross section for scattering of H by H_2[18] then immediately gave the absolute differential scattering cross section, which upon reinsertion into bracket term in Eq. (10) gave the absolute cross section calibration shown in Fig. 5. It is important to note that the absolute value scale so obtained is not the <u>true</u> total cross section for the scattering of both particles but the absolute <u>effective</u> cross section when using an electron-impact ionization detector.

Calibration of the reactive scattering cross section becomes possible upon determination of the apparatus constants, $Kn_1n_2V\Omega_D$, through the use of Eq. (10). In practice, the procedure was to measure the ratio of the reaction product signal and the scattered mass 2 signal, without explicit evaluation of the apparatus constants.

The differential reactive scattering cross section obtained under the assumptions made is given by

$$\frac{d\sigma(v)}{d\Omega} = (7.5 \pm 3.8)10^{-17} \left(1 - \frac{v_o^2}{v^2}\right) \cos^2 1.35(180^\circ - \theta), \quad (v \geq v_o) \text{cm}^2/\text{Sr}$$

$$= 0 \qquad , v < v_o \qquad (13)$$

and

$$\sigma(v) = \begin{cases} (3.5 \pm 1.8) \times 10^{-16} \left(1 - \frac{v_o^2}{v^2}\right) & , v \geq v_o \\ 0 & , v < v_o \end{cases} \qquad (14)$$

The specified uncertainty reflects only repeatability of the ratio of reactive HD to mass 2 signals. The calibrated laboratory differential scattering cross section is shown in Fig. 3.

The rate constant corresponding to this cross section is 1.2 ± 0.6 x 10^{-11} cm^2/sec. This bulk rate is calculated by inserting Eq. (14) into Eq. (15) and using the effective kinetic temperature for the present experiment, $T_B = 1400°K$.

$$k(T_B) = \int_0^\infty \sigma(v) v f(v) dv \qquad (15)$$

where

$$f(v) = \frac{4}{\sqrt{\pi}} \alpha^{3/2} v^2 e^{-\alpha v^2} \qquad \alpha = \frac{\mu}{2KT_B}$$

and μ is the reduced mass of the reactants.

Extrapolation of the lower temperature rate constant measurements of LeRoy, Ridley and Quickert[9d], to the effective temperature in the present experiments gives a value of 5.6 x 10^{-12} cm^3/sec. Considering the inherent uncertainties in the simple model used in discussion the present experimental results and the uncertainties of extrapolating the lower temperature data to the effective temperature of the crossed beam experiment, the discrepancy between the two rate coefficient values is remarkably small.

VI. CONCLUSION

The experimental reactive differential cross section for D + H_2 unquestionably verifies microscopic theoretical predictions that near threshold, reactively formed HD receeds from the collision with an anisotropic center-of-mass distribution that peaks roughly 180 degrees from the general direction of the attacking D atom. This angular distribution coupled with HD recoil velocity measurements which indicates that the D-H-H reacting configuration is short lived compared to rotational times also confirms that the HD prefers to leave the collision with little or no internal energy. The estimate of the total reactive cross section is in satisfactory agreement with extrapolated bulk rate data and is consistent with semi-classical prediction.

Detailed comparison of the experimental and theoretical differential cross sections indicates disagreement over the width of the HD angular distribution in the center-of-mass. This disagreement is not surprising considering the rather short period of time that theory and experiment have had to interact concerning microscopic details. Certainly we should look forward to the publication of more theoretical studies and to the data of more refined hydrogen reaction experiments before attempting to accurately assess the degree of theoretical understanding for this fundamental reaction.

ACKNOWLEDGMENTS

The authors are indebted to Dr. Sheldon Datz of the Oak Ridge National Laboratory and Prof. M. Karplus of Harvard University for generous discussion and correspondence regarding these experiments, and to Prof.

R. T. Brackmann for technical advice and assistance. One of us (WLF) is also indebted to the Air Force Office of Scientific Research and to Dr. J. F. Masi of that office for support of an earlier attempt at a similar experiment, in which many of the experimental techniques used in the present experiment were developed.

REFERENCES

1. E. H. Taylor and S. Datz, J. Chem. Phys. 23, 1711 (1955).

2. For a recent review see D. R. Herschbach in Advances in Chemical Physics, Vol. X, J. Ross Ed. (Interscience Publishers, New York, 1966).

3. S. Datz and E. H. Taylor, J. Chem. Phys. 39, 1896 (1963).

4. W. L. Fite and R. T. Brackmann, Atomic Collision Processes, M. R. C. McDowell, Ed., (North Holland Publ. Co., Amsterdam, 1964), pp. 955-963.

5. (a) Y. T. Lee, J. D. McDonald, P. R. Le Breton and D. R. Herschbach, J. Chem. Phys. 49, 2447 (1968).
   (b) J. Grosser and H. Haberland, Chem. Phys. Letters 7, 442 (1970).
   (c) D. Beck and H. Forster, Sixth International Conference on the Physics of Electronic and Atomic Collisions, Cambridge, Mass. 1969, M.I.T. Press (1969), pp. 587.
   (d) J. B. Cross and N. C. Blais, J. Chem. Phys. 50, 4108 (1969).

6. (a) M. Karplus and K. T. Tang, Discussions of Faraday Soc. 44, 56 (1967).
   (b) M. Karplus, R. N. Porter and R. D. Sharma, J. Chem. Phys. 43, 3259 (1965).
   (c) K. T. Tang and M. Karplus, J. Chem. Phys. 49, 1676 (1968).

7. D. A. Micha, Ark. Fysik 30, 437 (1965).
   30, 425 (1965).

8. A. Farkas and L. Farkas, Proc. Roy. Soc. (London) A152, 124 (1935).

9. (a) W. R. Schulz and D. J. LeRoy, Can. J. Chem. 42, 2480 (1964).
   (b) W. R. Schulz and D. J. LeRoy, J. Chem. Phys. 42, 3869 (1965).
   (c) B. A. Ridley, W. R. Schulz and D. J. LeRoy, J. Chem. Phys. 44, 3366 (1966).
   (d) D. J. LeRoy, B. A. Ridley and K. A. Quickert, Disc. Faraday Soc. 44, 92 (1967).
   (e) A. A. Westenberg and N. de Hass, J. Chem. Phys. 47, 1393 (1967).

10. L. A. Melton and R. G. Gordon, J. Chem. Phys. 51, 5449 (1969).

11. A. Kupperman and J. M. White, J. Chem. Phys. 44, 4352 (1966).

12. J. Geddes, H. F. Krause and W. L. Fite, J. Chem. Phys. 52, 3296 (1970).

13. H. Harrison, W. L. Fite and D. G. Hummer, J. Chem. Phys. 41, 2567 (1964).

14. S. Datz, D. R. Herschbach and E. H. Taylor, J. Chem. Phys. 35, 1549 (1964).

15. T. T. Warnock and R. B. Bernstein, J. Chem. Phys. 49, 1878 (1968).

16. R. K. Helbing, J. Chem. Phys. 48, 472 (1968).

17. S. Datz, private communication (1970).

18. H. Harrison, J. Chem. Phys. 37, 1166 (1962).

19. A. Dalgarno and R. J. Henry, Atomic Collisions Phenomena, M. R. C. McDowell, Ed. (North Holland Publ. Co., Amsterdam, 1964).

20. R. B. Bernstein, in Advances in Chemical Physics, Vol. X., J. Ross Ed. (Interscience Publishers, New York, 1966).

FIGURE CAPTIONS

Fig. 1. Velocity vector diagram for HD formed in the reaction $D + H_2 \to HD + H$ and for scattering of undissociated HD impurity in the D atom beam.

Fig. 2. Schematic for the crossed beam experiment.

Fig. 3. Angular distribution of reactively scattered HD.

Fig. 4. Velocity vector diagram showing the measured HD velocities. Also shown is the predicted elastically scattered HD impurity velocities.

Fig. 5. Angular distribution of the sum of the elastic scattering of D on H_2 and H_2 on D.

Fig. 6. Comparison of the experimental data with the calculated laboratory distribution for a C. M. angular distribution of the form $\cos^N M(180^\circ - \theta)$.

Fig. 7. Comparison of the experimental C. M. Angular distribution with theory. Distributions considered in the experimental analysis are of the functional form $\cos^N M(180^\circ - \theta)$.

Fig. 8. Comparison of the present experimental results with those of Datz and Taylor.

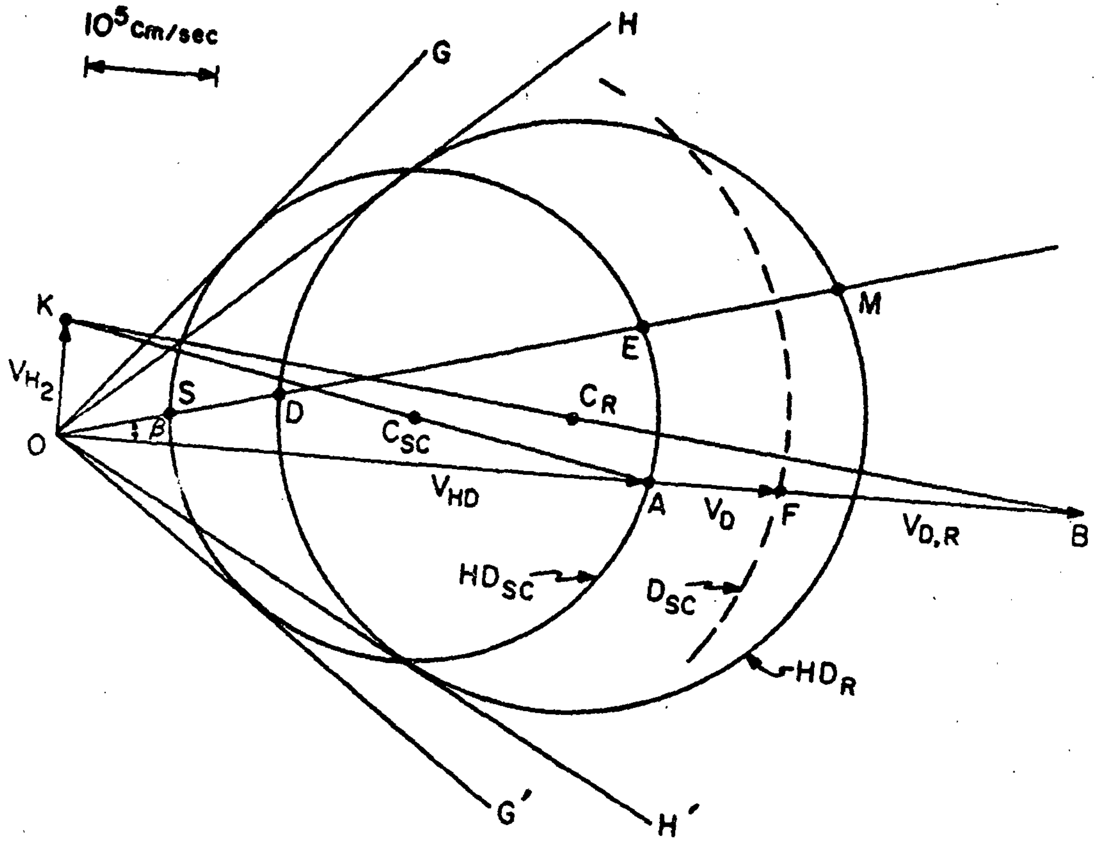

10^5 cm/sec
G
H
K
V_{H_2}
S
D
E
M
C_R
C_{SC}
O
β
V_{HD}
A
V_D
F
$V_{D,R}$
B
HD_{SC}
D_{SC}
HD_R
G′
H′

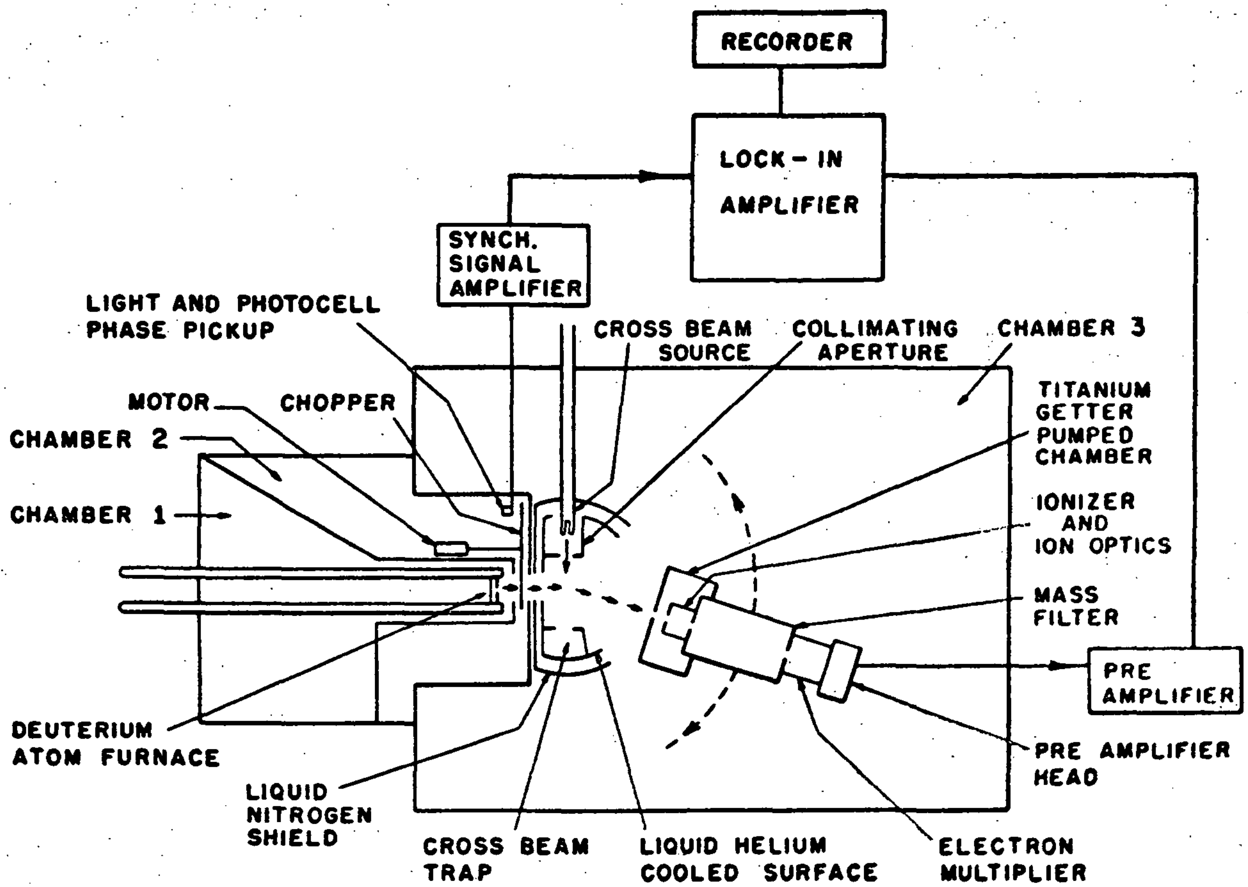
RECORDER
LOCK - IN AMPLIFIER
SYNCH. SIGNAL AMPLIFIER
LIGHT AND PHOTOCELL PHASE PICKUP
CROSS BEAM SOURCE
COLLIMATING APERTURE
CHAMBER 3
MOTOR
CHOPPER
CHAMBER 2
CHAMBER 1
TITANIUM GETTER PUMPED CHAMBER
IONIZER AND ION OPTICS
MASS FILTER
PRE AMPLIFIER
DEUTERIUM ATOM FURNACE
PRE AMPLIFIER HEAD
LIQUID NITROGEN SHIELD
CROSS BEAM TRAP
LIQUID HELIUM COOLED SURFACE
ELECTRON MULTIPLIER

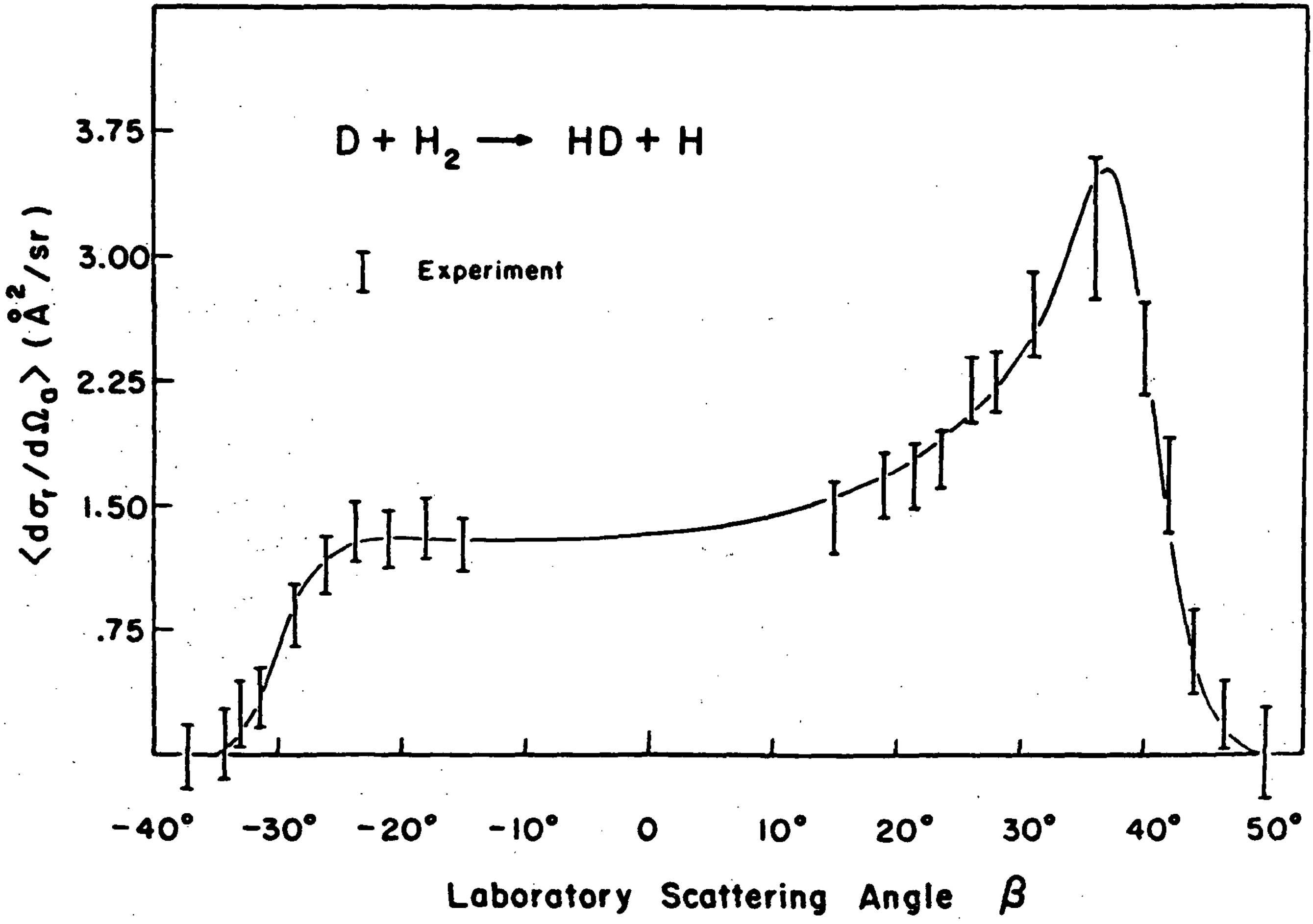
$D + H_2 \longrightarrow HD + H$
Experiment
3.75
3.00
2.25
1.50
.75
$\langle d\sigma_r / d\Omega_a \rangle$ ($\mathring{A}^2$/sr)
-40°
-30°
-20°
-10°
0
10°
20°
30°
40°
50°
Laboratory Scattering Angle β

$D + H_2 \rightarrow HD + H$

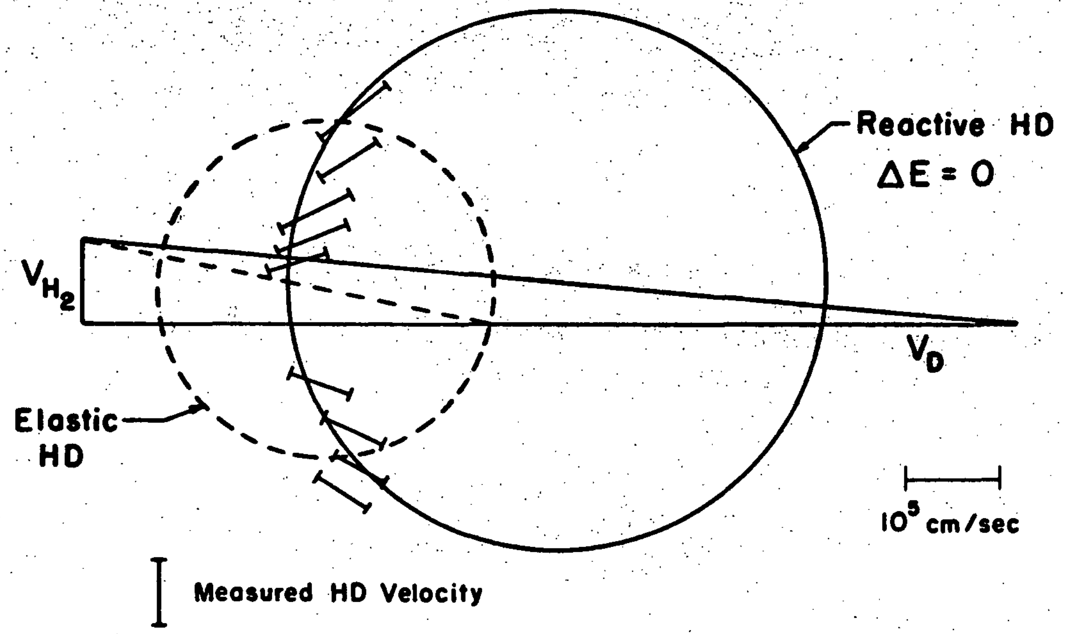

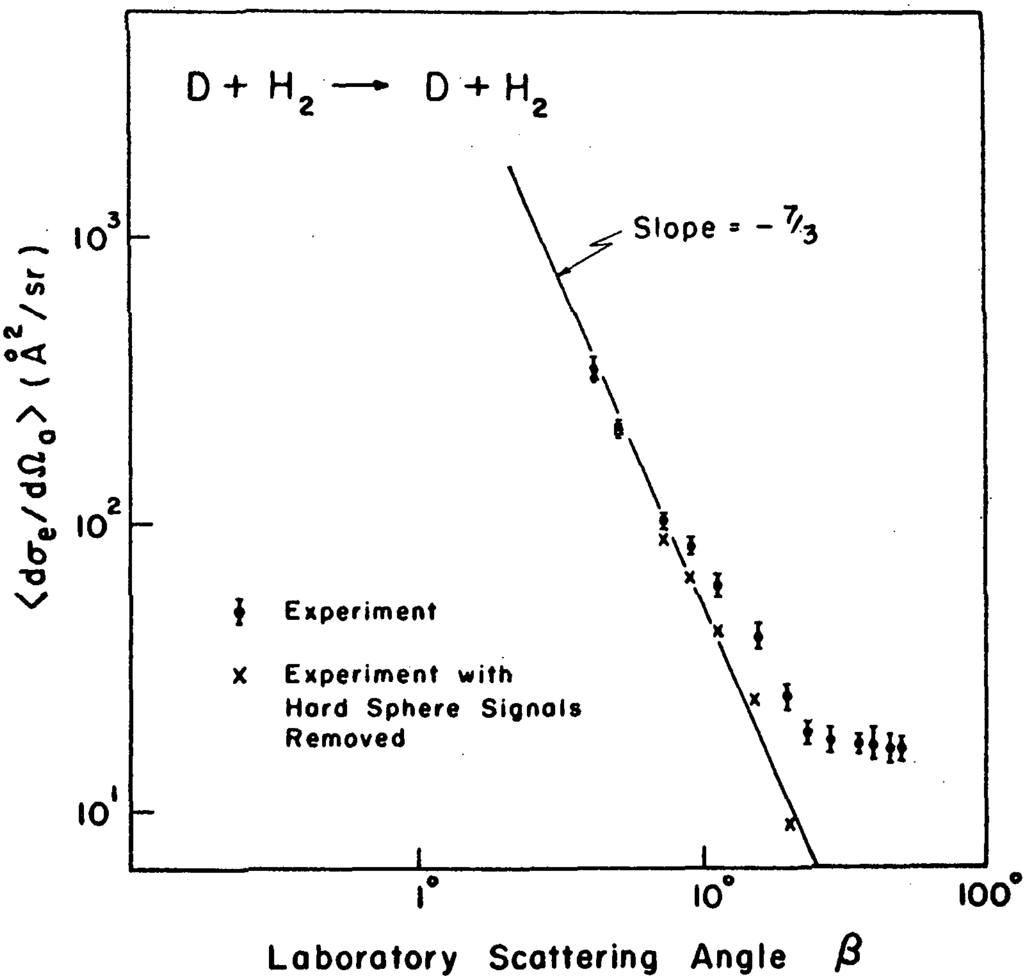

$D + H_2 \longrightarrow D + H_2$
Slope = $-7/3$
$\langle d\sigma_e/d\Omega_a \rangle$ (Å^2/sr)
10^3
10^2
10^1
Experiment
Experiment with Hard Sphere Signals Removed
1°
10°
100°
Laboratory Scattering Angle β

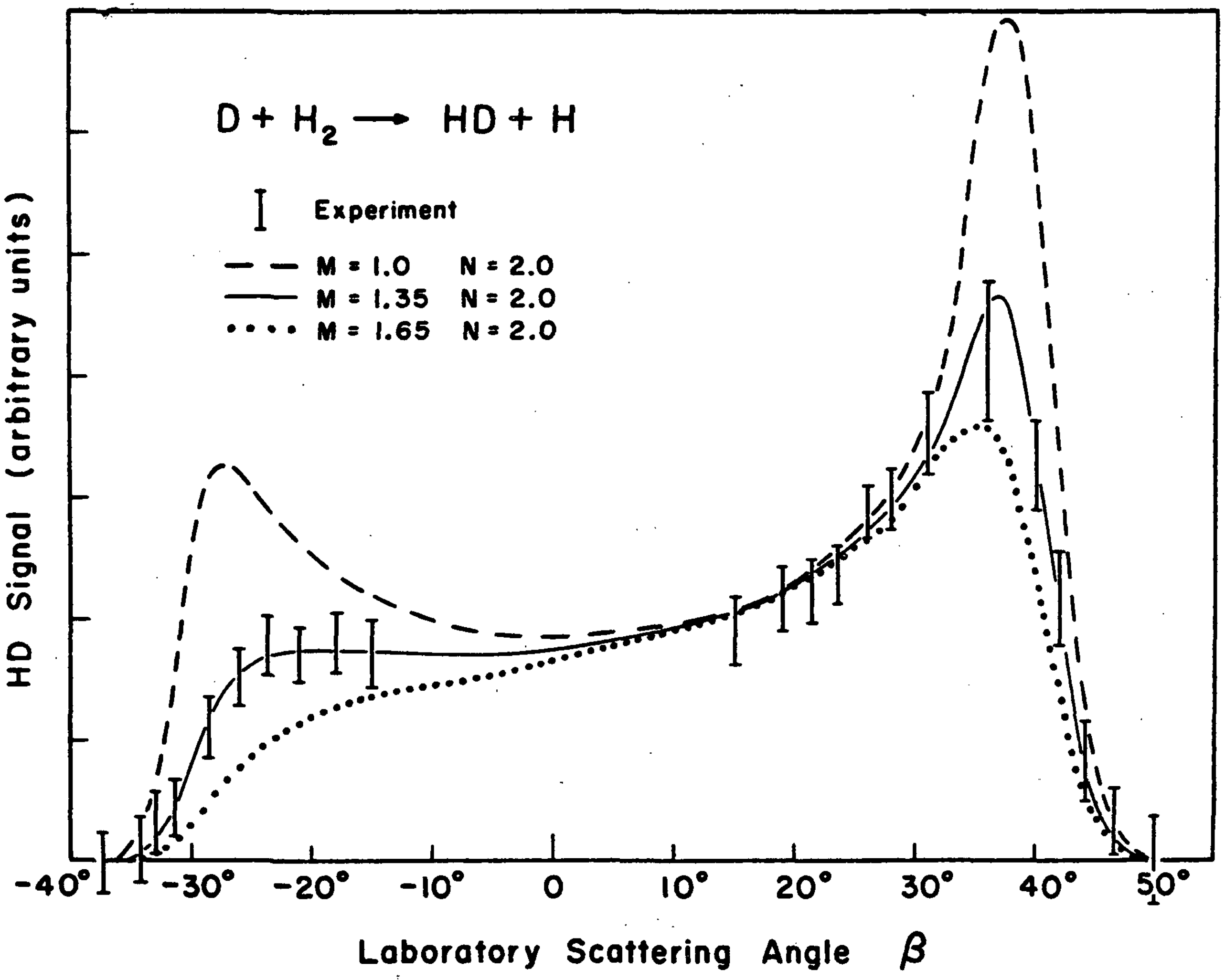
D + H_2 ⟶ HD + H
Experiment
M = 1.0 N = 2.0
M = 1.35 N = 2.0
M = 1.65 N = 2.0
HD Signal (arbitrary units)
-40°
-30°
-20°
-10°
0
10°
20°
30°
40°
50°
Laboratory Scattering Angle β

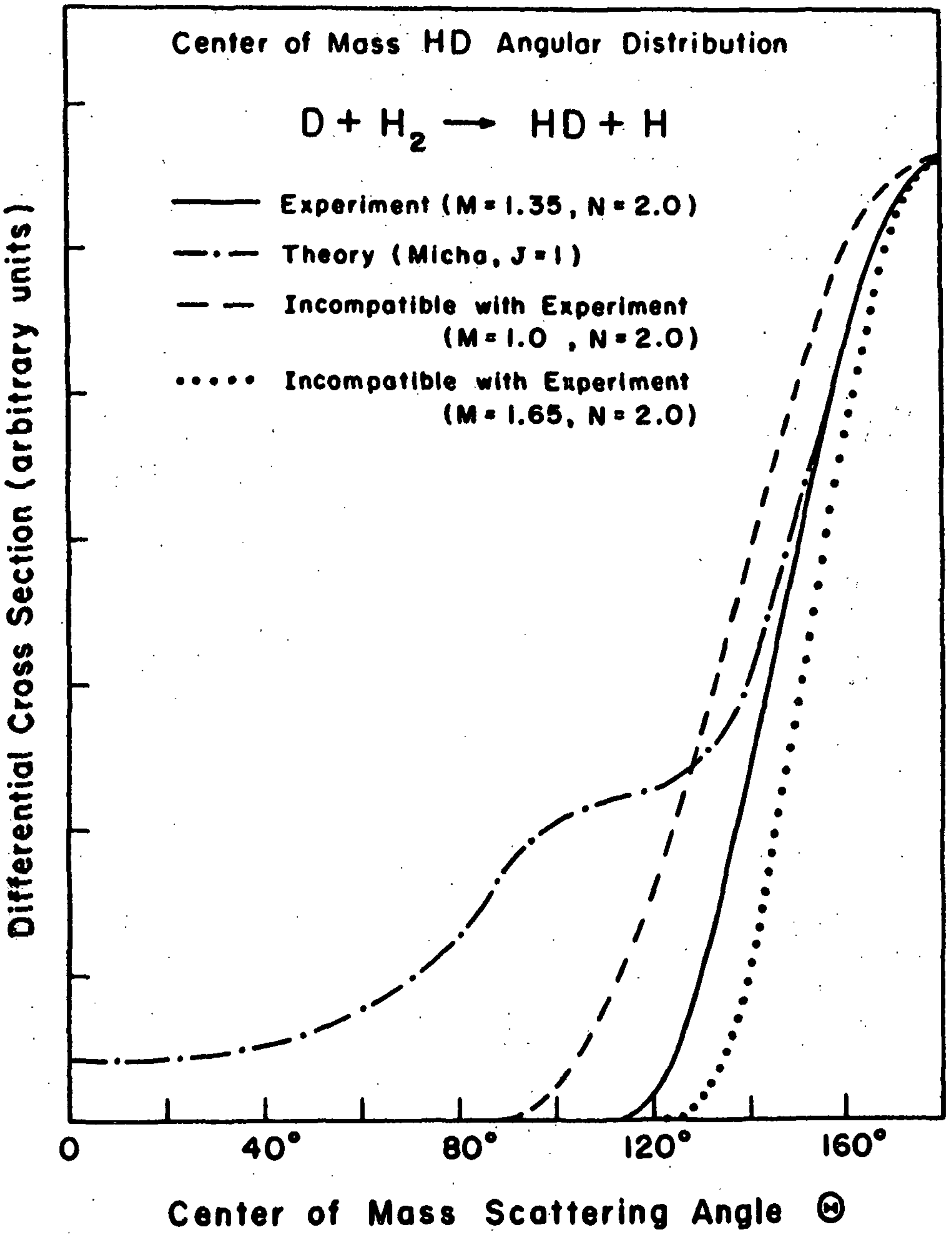
Center of Mass HD Angular Distribution
$D + H_2 \longrightarrow HD + H$
Experiment (M = 1.35, N = 2.0)
Theory (Micha, J = 1)
Incompatible with Experiment (M = 1.0 , N = 2.0)
Incompatible with Experiment (M = 1.65, N = 2.0)
Differential Cross Section (arbitrary units)
0
40°
80°
120°
160°
Center of Mass Scattering Angle Θ

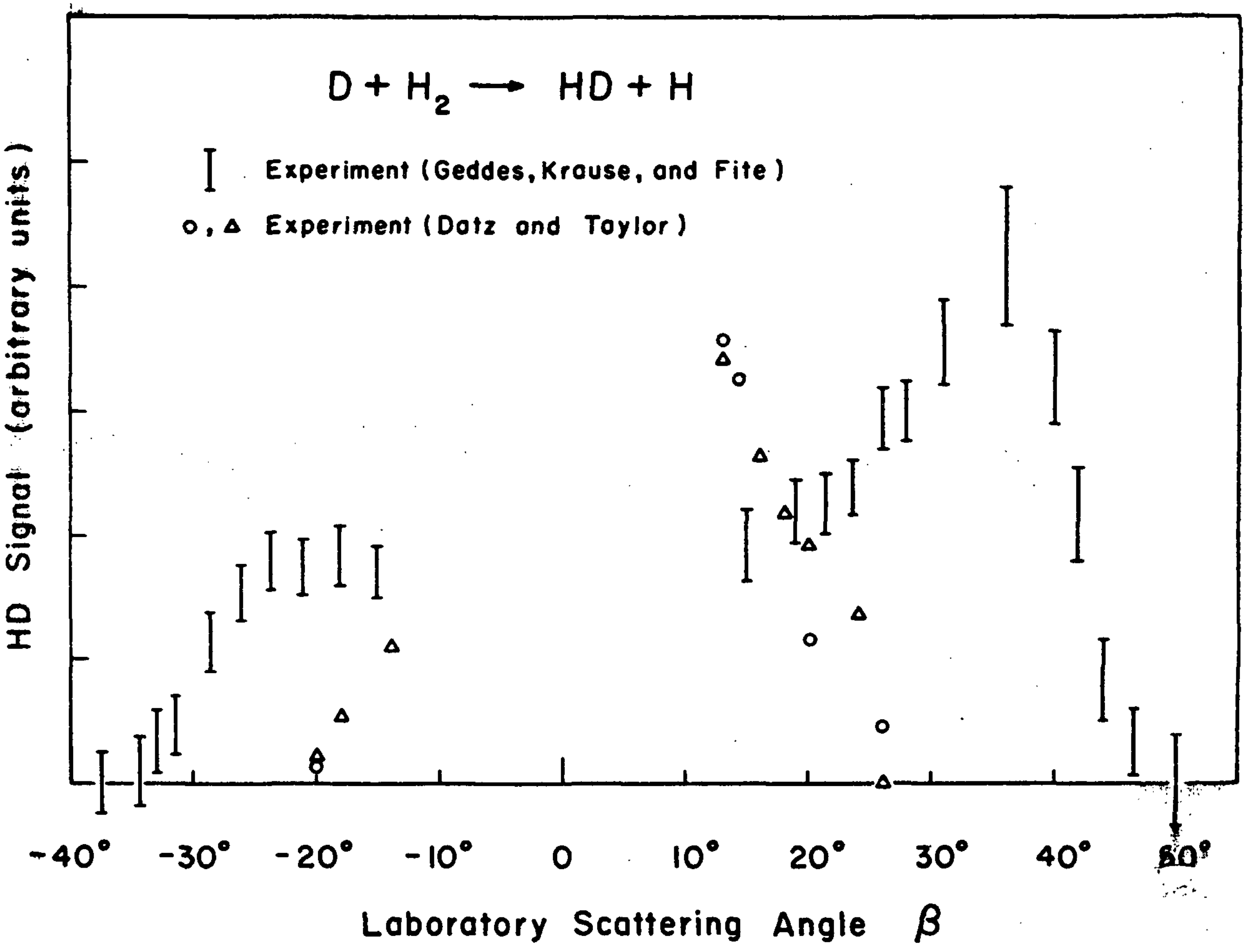

$D + H_2 \longrightarrow HD + H$
Experiment (Geddes, Krause, and Fite)
○, △ Experiment (Datz and Taylor)
HD Signal (arbitrary units)
-40°
-30°
-20°
-10°
0
10°
20°
30°
40°
50°
Laboratory Scattering Angle β